A New Dispersion Interferometer for the Stellarator Wendelstein 7-X

J. Knauer, P. Kornejew, H. Trimiño Mora, M. Hirsch, A. Werner, R.C. Wolf

and the W7-X Team

Max-Planck-Institut für Plasmaphysik, Greifswald, Germany

I. Introduction

A single channel dispersion interferometer (DI)[1] was installed on the stellarator Wendelstein 7-X (W7-X) for electron density measurements. It has been operated during the first operation campaign (OP1.1) and provides time traces of the line integrated electron density. In this paper, measurements of the DI during two month operation are presented. First results indicate a good particle confinement of the stellarator 7-X, because the electron density remains at high level even after the heating (by ECRH) has been switched off.

II. Dispersion Interferometry

The principle set-up of a dispersion interferometer is shown in fig. 1. Before entering the plasma, a frequency doubled laser beam is generated from the fundamental laser beam by means of a frequency doubling crystal (FDC). Both beams cross the plasma with different group velocities due to their different wavelength. Afterwards they pass the FDC a second time.

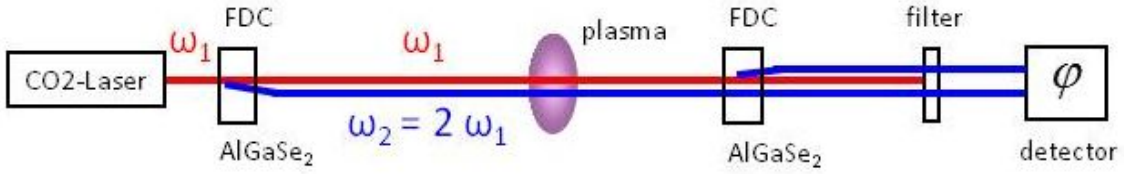

Fig. 1: Principle of dispersion interferometry

The phase of the radiation which passes the plasma is changed due to the plasma electrons according to

$$\frac{\lambda e^2}{4\pi c^2 \varepsilon_0 m_e} \int n_e(l)\, dl\,,$$

where e is the elementary charge, c the speed of light, m_e the mass of the electron, ε_0 the dielectric constant of vacuum, n_e the electron density of the plasma and λ the wavelength of the electromagnetic wave. The integral is taken over the path l through the plasma. In front of the detector a filter removes the fundamental wavelength. At the detector, the interference signal of both frequency doubled beams is detected, which has the intensity

$$I = A_1^2 + A_2^2 + 2A_1A_2\cos(\Delta\varphi),$$

where A_1^2 and A_2^2 are the intensities of the two interfering beams and $\Delta\varphi = \varphi_1 - \varphi_2$ is the phase difference between them, with:

$$\varphi_1 = 2\omega t + 2\frac{2\pi}{\lambda_L}\Delta z + \varphi_{1,\mathrm{mod}} + \frac{(\lambda_L/2)e^2}{4\pi c^2 \varepsilon_0 m_e}\int n_e(l)\, dl\,,$$

$$\varphi_2 = 2\left(\omega t + \frac{2\pi}{\lambda_L}\Delta z + \varphi_{2,\mathrm{mod}} + \frac{\lambda_L e^2}{4\pi c^2 \varepsilon_0 m_e}\int n_e(l)\, dl\right).$$

λ_L is the fundamental wavelength of the laser and Δz denotes the geometrical changes of the beam path (e.g. due to vibrations). $\varphi_{n,mod}$ are applied phase shifts due to modulation of the signal in order to apply a heterodyne detection scheme. $\Delta\varphi$ does not depend on geometrical changes of the beam path anymore delivering for the final phase change

$$\Delta\varphi = \varphi_2 - \varphi_1 = \Delta\varphi_{\mathrm{mod}} + \frac{3}{2}\frac{\lambda_L e^2}{4\pi c^2 \varepsilon_0 m_e}\int n_e(l)dl.$$

This means that dispersion interferometers are intrinsically insensitive to changes of the geometrical path length, e.g. caused by vibrations, because both beams follow exactly the same beam path. Only vibrations perpendicular to the beam path leading to a misalignment would increase the phase noise.
Another big advantage of the dispersion interferometer set-up is that a reference beam path, as necessary for other interferometer set-ups (like Michelson or Mach-Zehnder), is no longer needed. Therefore, different conditions in reference and plasma beam path (e.g. due to vibrations, air convection and humidity) cannot affect the signal to noise ratio of the measured phase shift.

III. Layout at W7-X

The dispersion interferometer at W7-X[2] is based on a 20W CO_2 laser and its second harmonic, which is generated by an $AgGaSe_2$ frequency doubling crystal. The efficiency of the FDC is rather low, producing second harmonic intensity with a fraction of only some 10^{-6}. Both beams pass the plasma vessel twice being back reflected by a corner cube reflector (CCR) which is located outside the vacuum vessel on the inner side of the torus. Thus the phase shift due to plasma electrons is doubled. The lateral distance between the incident and the reflected beams is chosen to be 35 mm to avoid perturbations of the laser operation by reflection of 10.6µm radiation back into the laser. After frequency doubling of a small part of the residual 10.6 µm beam in a second $AgGaSe_2$ crystal, the phase shift of the two 5.3 µm signals is detected. A single beam path within the plasma is approximately 1.33 m (depending on the magnetic configuration).

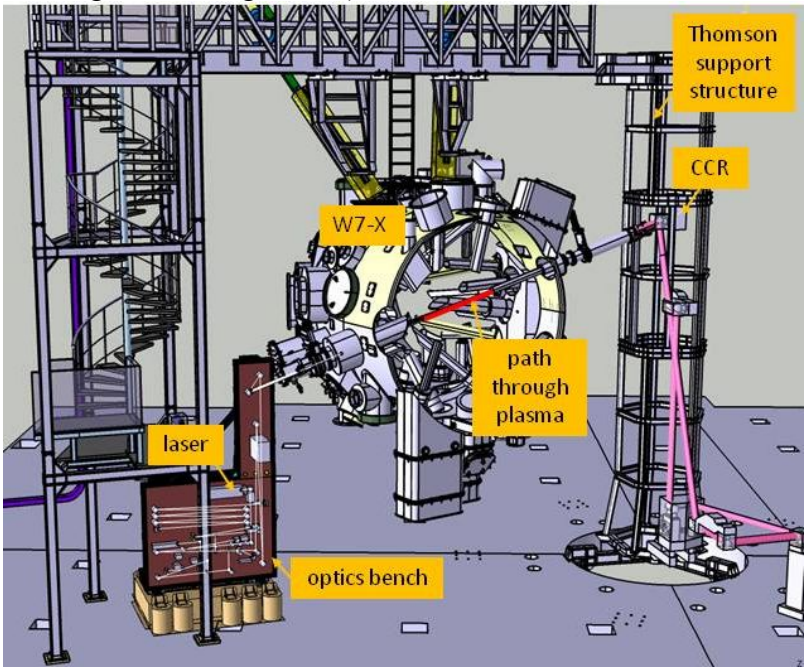

Fig. 2: Layout of the interferometer set-up. The W7-X plasma vessel is not shown.

The phase measurement uses a heterodyne modulation scheme applying a photoelastic ZnSe modulator (PEM) at a modulation frequency of 50 kHz to the 5.3µm signal which also determines the temporal resolution. The plasma induced phase shift is derived from the interference of the returning signals, sampled at 50MS/s followed by phase comparison with the 50 kHz modulation signal, decimation and digital filtering by means of a Field

Programmable Gate Array (FPGA), which provides data in real time. However, for this first campaign the time resolution of the time trace transferred to the data base has been restricted to the time scale requested for later density feedback i.e. 1 ms. The single channel DI interferometer shares its sightline with the Nd:YAG-laser of the Thomson scattering system, therefore cross-calibration with the Thomson scattering system can be easily performed.

IV. Operation and Results

Time traces of the line integrated electron density were measured for all W7-X discharges in the first operation campaign OP1.1. The measurement of the longest discharge (6 s) is shown in fig. 3. The derived noise level is slightly below 10^{17} m^{-2}. The analysis algorithm worked well for values up to $6 \cdot 10^{19}$ m^{-2}, if the initial phase at zero density is selected well.

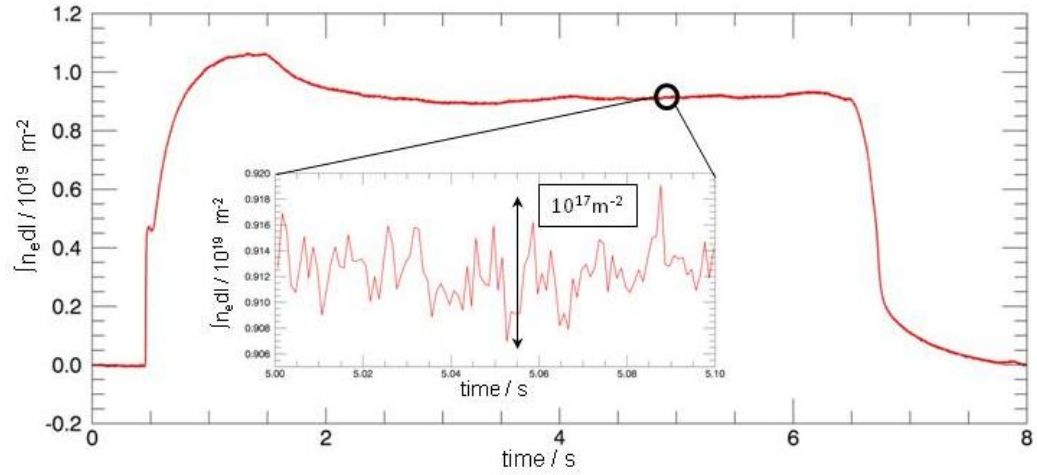

Fig. 3: Time trace for 6s hydrogen discharge 20160310#10. Noise level is lower than 10^{17} m^{-2}.

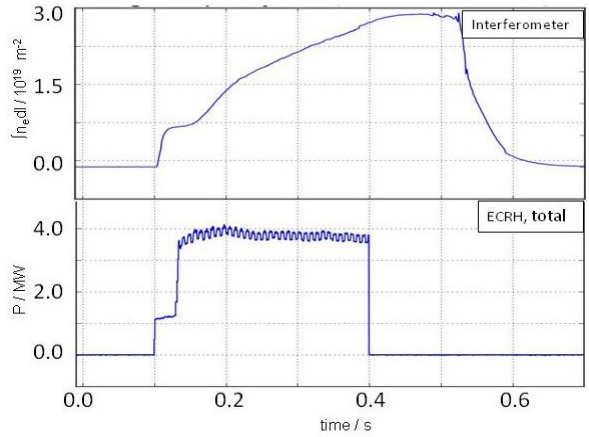

Fig. 4: Time traces of line integrated electron density (upper) and total ECRH heating power (lower) for helium discharge 20160202 #19.

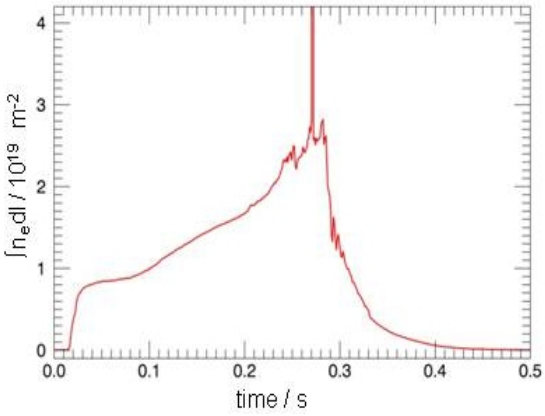

Fig. 5: Time trace for hydrogen discharge 20160204 #18. The initial phase was not adjusted well.

In fig. 4 the line integrated density is shown together with the (modulated) total electron cyclotron resonance heating (ECRH) power. It can be seen that the line integrated density remains at a high level for more than 100 ms after the heating power has been switched off, which is an indication for a long particle confinement time (and a remaining particle source). In contrast, the electron temperature starts to drop down on a shorter time scale after switching off the heating power (ECE measurements[3], not shown).

To fully exploit the dynamic range of the diagnostic it was necessary to adjust the initial phase of the system continuously, because it changed during the experimental day, probably

caused by temperature effects. Therefore, for long pulse operation it is necessary to put additional effort into the cooling of the optical components of the set-up. E.g. the FDCs have to meet the requirements of longer discharges (when all in-vessel components are actively cooled, discharges of up to 30 minutes are planned).
The phase was adjusted by tilting the second FDC by means of a motorized optical mount. This worked quite well, but tilting the crystal also affects its conversion-efficiency. Therefore, it also has a pronounced effect on the signal strength. Moreover, there is a risk that the crystal is damaged when tilting it too far, as too much power is absorbed at its side surfaces. Fig. 5 shows an example of a case where the initial phase is not adjusted well, restricting the dynamic range of the system to lower values. Here, at $2.5 \cdot 10^{19}$ m^{-2} the noise increases significantly and even a misinterpretation of the signal occurs (seen as spike in the signal). This problem happens if the overall phase goes through 2π.

V. Planned Extensions

Extensions of the interferometer set-up are planned to allow for measurements of 30 min discharges. A feedback controlled beam steering system will be installed to maintain the alignment of the laser beams on their way through the plasma to the CCR and back to the interferometer. It consists of two four-quadrant diodes together with two motorized mirror mounts controlled by a PLC unit (Siemens SIMATIC). This system has been already tested under laboratory conditions. The correction of slow phase drifts (timescale larger than seconds) resulting in a baseline drift of the density by some 10^{18} m^{-3} is also relevant. This may be caused by air convection modulating the refraction index along the beam path. Therefore the number of water-cooled components of the optical set-up will be extended, including both FDC mounts. Additional temperature sensors will be installed for the monitoring of temperature characteristics at several places. For correcting of the initial phase of the system a wedged ZnSe plate will be installed on a motorized linear stage in the beam path. Therefore, tilting of the second FDC for phase correction (which also affects performance of the system, as mentioned) will be no longer needed. The FPGA data analysis routine will be further developed to enhance the dynamical range of the interferometer, such that a reliable determination of line integrated density values larger than $6 \cdot 10^{19}$ m^{-2} can be guaranteed. Furthermore, it will be possible to vary the cooling water temperature of the laser chiller remotely.
The interferometer is planned to be used for density control of W-7X in the next experimental campaigns. Besides this, a density feedback control loop will be installed, also using the interferometer data as an interlock to protect the in-vessel components from damage by plasma heating systems.

ACKNOWLEDGEMENT

This work has been carried out within the framework of the EUROfusion Consortium and has received funding from the Euratom research and training programme 2014-2018 under grant agreement No 633053. The views and opinions expressed herein do not necessarily reflect those of the European Commission.

References

[1] V. P. Drachev et al., Rev.Sci. Instrum. 64 (4), 1010 (1993)
[2] P. Kornejew et al., *Single channel dispersion interferometer for the Stellarator Wendelstein 7-X*, to be published in Rev. Sci. Instruments
[3] M. Hirsch et al., *ECE measurements in Wendelstein 7-X plasmas*, P4.007 (this conference)